LA-10553

UC-34A
Issued: January 1986

LA--10553

DE86 007586

Free-Free Gaunt Factors: Comparison of Various Models

L. A. Collins
A. L. Merts

Los Alamos National Laboratory
Los Alamos, New Mexico 87545

GLOSSARY OF ACRONYMS

AAFEGE	asymptotically adjusted free-electron gas-exchange
CC	close-coupling
FC	frozen-core
FEG	free-electron gas
HF	Hartree-Fock
HFEGE	Hara free-electron gas-exchange
IE	integral equations
IIE	iterative integral equations
LA	linear algebraic
S	static
SE	static-exchange
SEP1a	static-exchange model polarization (exponential-six cutoff)
SEP1b	static-exchange model polarization (cutoff term to sixth power)
SEP2	static-exchange model polarization (FEG)
SS	screened static
2CC	two-state close-coupling

FREE-FREE GAUNT FACTORS: COMPARISON OF VARIOUS MODELS

by

L. A. Collins and A. L. Merts

ABSTRACT

We develop the general theory of free-free absorption processes in terms of basic quantum mechanical principles. We perform calculations of the free-free Gaunt factor for several models of the electron-atom (ion) interaction in a variety of systems including rare gases, alkali, and aluminum. In addition, we investigate plasma-screening effects in such models as the Yukawa potential. Our calculations compare well with those of other authors, and our comparative study of various models allows a more thorough understanding of their range of validity.

I. GENERAL FORMULATION

The free-free absorption or inverse Bremsstrahlung process is described by the following mechanism:

$$h\nu + e^- E + A \rightarrow e^- E' + A \quad ,$$

where E (E′) is the initial (final) energy of the continuum electron, $h\nu(=\hbar\omega)$ is the energy of the photon, and A represents an atomic or ionic target. This radiative mechanism has been investigated extensively, and a representative, though by no means exhaustive, survey is given in the first set of references.[1-13]

The process is usually characterized in terms of an absorption coefficient $a(E,\omega)$[2,3,14], which relates the number of absorptions by electrons per unit volume per unit time, k_{ff}, to the number density of free electrons (n_e) and of atoms (n_i), the normalized electron distribution f(E)dE, and the Planck radiation flux Pd(hν):

$$k_{ff} = n_i n_e \, a(E,\omega) \, f(E)dE \, P\frac{d(h\nu)}{h\nu} \quad . \tag{1}$$

The Planck radiation flux is related to the radiation energy density U by the speed of light c and is given by

$$Pd(h\nu) = 8\pi \frac{\nu^3}{c^2}[\exp(-h\nu/kT) - 1] \, d(h\nu) \quad [\text{ergs/cm}^2 \text{ sec}] \quad . \tag{2}$$

For a Maxwell-Boltzmann distribution of the electrons, we have

$$f(E)dE = \frac{2}{\pi^{1/2}}(k_B T)^{-3/2} \exp(-E/k_B T) \, E^{1/2} \, dE \quad , \tag{3}$$

where T is the electron temperature in degrees Kelvin (°K), E is the kinetic energy of the electron ($\frac{1}{2}mv^2$) with v (m) the electron velocity (mass), and k_B is the Boltzmann constant.

The absorption coefficient in units of cm^5 is in turn related to a dimensionless quantity $g(E,\omega)$, called the Gaunt factor, through the expression

$$a(E,\omega) = \sigma_K \, g(E,\omega) \ . \tag{4}$$

The scaling term σ_K is the Kramer's form of the semiclassical free-free absorption coefficient for an electron interacting with a point charge Ze and is given by[15]

$$\sigma_K \equiv \frac{4\pi Z_c^2 e^6}{3\sqrt{3}\, m^2 c h \nu \nu^3} \qquad [cm^5] \ . \tag{5}$$

This construction is simply a convention whereby the absorption coefficient reduces to its proper semiclassical limit when the Gaunt factor approaches unity ($a \to \sigma_K$ when $g \to 1$). This convention proves useful in many cases since, even for more detailed quantum mechanical treatments of the free-free process, the Gaunt factor remains close to one. One additional point is worth noting: we have used the symbol Z_c rather than Z to denote the charge that appears in σ_K and in g [see Eq. (11)]. We make this distinction since the resulting absorption coefficient, a, is independent of this choice ($a = \sigma_K g$; $\sigma_K \propto Z_c^2$ and $g \propto Z_c^{-2}$). In fact, for a neutral system, the quantity Z_c has no apparent meaning and is irrelevant to the calculation of a. For comparison among various models within the same calculational scheme, we generally set $Z_c = 1$, whatever the species under consideration. Care must be exercised in comparing Gaunt factors for ionic systems calculated by different authors since Z_c may reflect other conventions.

For most applications, the quantity of greatest interest is the absorption coefficient averaged over a particular electron distribution:

$$\bar{a}(T,\omega) = \frac{\int_0^\infty a(E,\omega) f(E) dE}{\int_0^\infty f(E) dE} \ , \tag{6}$$

where we recall that E is the electron energy, T is the electron temperature, and ω is the frequency of the radiation field.

For a Maxwell-Boltzmann distribution [Eq.(3)], we have[16]

$$\bar{a}(T,\omega) = \frac{4\pi Z_c^2 e^6}{3\sqrt{3}\, hcm^2\nu^3} \left(\frac{2m}{\pi k_B T}\right)^{1/2} \bar{g}(T,\omega) \quad [cm^5] \ , \tag{7}$$

where the averaged Gaunt factor $\bar{g}$ is given by

$$\bar{g}(T,\omega) = (k_B T)^{-1} \int_0^\infty g(E,\omega) \exp(-E/k_B T)\, dE \ . \tag{8a}$$

The averaged Gaunt factor is also related to the absorption coefficient per unit pressure per atom, κ, which is more common in astrophysical models:

$$\kappa = C_5 Z_c^2 (\Delta k^2)^{-3} \theta^{3/2} \bar{g} \quad [cm^4/dyn] \ , \tag{8b}$$

where Δk^2 is the photon energy in Rydbergs, $\theta = 5040/T$ (kelvins), and $C_5 = 2.0991 \times 10^{-28}$ (see Appendix A).

Another common quantity of interest is the effective mass absorption coefficient σ_{eff} (cm^2/g), which is related to the absorption coefficient by

$$\sigma_{eff} = \frac{N_o \bar{a}}{A} n_e \ , \tag{9}$$

where N_o is Avagadro's number, and A is the atomic weight of the target (g/mole). The effective absorption coefficient is important in considering the attenuation of radiation through a material. For the case of only free-free absorption, the intensity of radiation I, at radial distance X, compared with that at the origin I_o is given by

$$I = I_o \exp(-\tau X) \ , \tag{10}$$

where $\tau \equiv \rho \ \sigma_{eff}$ with ρ the mass density (g cm^{-3}).

The absorption coefficient can also be employed to determine the real part of the index of refraction, n, of a medium. In the case of sharp density gradients such as those encountered at the surface of a metal, the real part of n, or reflectivity, may be more important than the imaginary part related to absorption. The reflectivity, Re n, can be determined from formulae given by Griem[17] [see Eqs.(14-2) and (14-3) and the discussion on p. 551 in Griem1. In many cases, however, this quantity can be obtained more readily from direct experimental measurements.

II. FREE-FREE GAUNT FACTOR

A. General Form

In our case, we calculate the free-free Gaunt factor from quantum mechanical considerations. For scattering from a central potential, from a ground-state closed-shell target, or from an atom or ion with a single s-electron outside a closed shell, the free-free Gaunt factor has the form (see Appendices A and B)*

$$g(E,\omega) = \frac{2\sqrt{3}\,\omega^4 m^2}{Z_c^2 \pi\, e^4 k k'} M_L \ , \tag{11}$$

where

$$M_L = \sum_{\ell\ell'}^{\ell_m} \ell_{max}\, d^L_{\ell\ell'}(k|k')^2 \ , \tag{12}$$

In these equations, k is the wavenumber [$k = (2mE/\hbar^2)^{1/2}$], ℓ is the orbital angular momentum of the continuum electron, ℓ_{max} is given by $\max(\ell,\ell')$, and $d^L_{\ell\ell'}$ is the dipole matrix element. More complicated coupling schemes are discussed by Sobelman.[15] Since g is a dimensionless quantity, we may express it equally well in atomic units ($e = \hbar = m_e = 1$; 1 a.u. of energy = 1 hartree = 27.212 eV):

$$g(E,\omega) = \frac{2\sqrt{3}\,\omega^4}{Z_c^2 \pi\, k k'} M_L \ . \tag{13}$$

The dipole matrix element in the length form (L) is given by

$$d^L_{\ell\ell'}(k|k') = \int f_{k\ell}(r)\, r f_{k'\ell'}(r) dr \ , \tag{14a}$$

where $f_{k\ell}(r)$ is the radial wavefunction for the continuum electron [see Eq.(17g)]. Another common expression for local potentials is the acceleration (A) form

$$d^A_{\ell\ell'}(k|k') = \int f_{k\ell}(r) \frac{d}{dr} V(r)\, f_{k'\ell'}(r) dr \ , \tag{14b}$$

---

*This form can also be used for scattering from a target consisting of a single s-electron outside a closed-shell, provided that $d_{\ell\ell'}$ is replaced by 1/4 [$d_{\ell\ell'}(S) + 3d_{\ell\ell'}(T)$], where S (T) stands for singlet (triplet) scattering.

where V(r), the interaction potential, is in hartrees. These two forms are simply related by

$$d^L = \omega^{-2} d^A(V) \ . \tag{15a}$$

Some authors express the acceleration form in terms of the potential U in Rydbergs (U = 2V), giving the relation

$$d^A(V) = \frac{1}{2} d^A(U) \ . \tag{15b}$$

A more common representation of the Gaunt factor is

$$g(E,\omega) = \frac{\sqrt{3}(\Delta k^2)^4}{8Z_c^2 \pi k k'} M_L \ , \tag{16a}$$

where the photon energy (Δk^2) and wavenumbers are expressed in Rydberg units. Similarly, we can write

$$g(E,\omega) = \frac{2\sqrt{3}}{Z_c^2 \pi k k'} M_A(V) \ , \tag{16b}$$

and

$$g(E,\omega) = \frac{\sqrt{3}}{2Z_c^2 \pi k k'} M_A(U) \ , \tag{16c}$$

where the latter is the expression used by Green.[16]

B. Continuum Solutions and Model Potentials

1. Scattering Formulation. The total-system wavefunction for an electron scattering from an N-electron atom (ion) solves the following Schrödinger equation[18-25]

$$H \psi(1 \ldots N+1) = E \psi(1 \ldots N+1) \ , \tag{17a}$$

where

$$H = H_o + V_{en} + V_{ee} + T \ .$$

In these equations, H_o is the Hamiltonian of the atom; V_{en} (V_{ee}) is the interaction of the incident electron with the nuclear charge (bound electrons) of the target; T is the kinetic energy of the scattered electron; and E is the total energy of the system. The notation $\psi(1 \ldots N+1)$ stands for the more involved representation $\psi(\tau_1 \ldots \tau_{N+1})$, where τ_i has both spatial $\vec{R}_i$ and spin σ_i coordinates. The wavefunction for a particular state, n, of the target atom satisfies the eigenvalue equation

$$H_o \Phi_n(1 \ldots N) = E_n \Phi_n(1 \ldots N) \ , \text{ and}$$

$$\langle \Phi_n | \Phi_{n'} \rangle = \delta_{nn'} \ . \tag{17b}$$

Equation (17a) is an (N+1)-body expression and is difficult to solve in this form. We reduce this equation to an effective one-particle equation by introducing an expansion of the total-system wavefunction ψ in terms of a complete set of target states of the form

$$\psi(1 \ldots N+1) = \sum_{n'} A[\Phi_{n'}(1 \ldots N) F_{n'}(N+1)] \ , \tag{17c}$$

where $F_{n'}(N+1)$ represents the continuum function and A is an antisymmetry operator, which guarantees that the product satisfies the Pauli restriction for fermions. We now substitute Eq. (17c) into Eq. (17a), multiply through by $\Phi_{n'}^{\dagger}(1...N)$ and the spin functions for the continuum electron, and integrate over all target coordinates $d\tau_1$, ... $d\tau_N$ and the spin of the scattered electron σ_{N+1} to derive the following expression for the continuum orbital F_n:

$$[T + (E_n - E)]\, F_n(\vec{R}_{N+1}) = \sum_{n'} V_{nn'}(\vec{R}_{N+1})\, F_{n'}(\vec{R}_{N+1}) \quad , \tag{17d}$$

where

$$V_{nn'}(\vec{R})\, F_{n'}(\vec{R}) \equiv \langle \Phi_n | V_{ee} + V_{en} | A(\Phi_{n'} F_{n'}) \rangle \quad .$$

Thus, we have reduced the many-body formulation to an effective one-particle equation whose solution is the wavefunction for the scattered electron. We note that Eq. (17d) involves coupling between all channels n'. However, in practice, we invoke the close-coupling (CC) approximation by which the infinite sum in Eq. (17d) is trancated at some small number of channels. We further reduce Eq. (17d) to a set of coupled, radial integrodifferential equations by (1) making a single-center expansion of the bound and continuum orbitals

$$F_n(\vec{R}) = \sum_{\ell'_n} R^{-1} f_{n\ell'_n}(R)\, Y_{\ell'_n m}(\hat{R}) \quad , \tag{17e}$$

where $Y_{\ell m}$ is a spherical harmonic, (2) multiplying through by $Y_{\ell_n m}^{*}(\hat{R})$, and (3) integrating over all angular coordinates $d\hat{R}$. The resulting set of coupled radial equations can be written in the abbreviated form

$$L_\alpha f_\alpha(R) - \sum_{\alpha'} \int W_{\alpha\alpha'}(R|R') f_{\alpha'}(R') dR' = 0 \quad , \tag{17f}$$

where

$$L_\alpha \equiv \frac{d^2}{dR^2} - \ell_n(\ell_n + 1)R^{-2} + k_n^2 \quad , \text{and}$$

$$k_n^2 = 2(E - E_n) \quad .$$

The channel label is given by $\alpha = (n\ \ell_n)$, where ℓ_n is the orbital angular momentum of the incident electron. The coupling potential $W_{\alpha\alpha'}$ is a complicated expression that is energy-dependent and nonlocal and has the general form

$$\int Y_{\ell_n m}^{*}(\hat{R}') V_{nn'} Y_{\ell_{n'} m'}(\hat{R}') d\hat{R}' \quad .$$

2. Static-Exchange (SE) Approximation. In general, we do not treat the full close-coupling equations [Eq. (17f)], but make some simplifying approximations: (1) that we consider only elastic scattering (n = n' = ground state of the target) and (2) that we treat only scattering from a local central potential, from a closed-shell target, or from an atom with a single s-electron outside a closed shell. The restriction to elastic scattering does not eliminate multichannel effects since the sum in Eq. (17f) runs over the closed electronic channels. These virtual excitations give rise to correlation and polarization effects and represent the distortion of the target atom by the incident electron. While we do not solve the CC equations for more than one channel, we do include these correlation effects in some cases by model potentials (see Section II.B.3).

For most cases, we neglect these virtual excitations and invoke the SE approximation whereby the target is frozen in its ground state but the Pauli principle is satisfied. Within these simplifying assumptions, the continuum function solves a single-channel Schrödinger equation of the form

$$L f_{k\ell}(R) = \int_0^\infty W(R|R')\, f_{k\ell}(R')\, dR' \quad , \tag{17g}$$

where

$$L \equiv \frac{d^2}{dR^2} + \ell(\ell+1)R^{-2} + k^2 \quad ,$$

ℓ is the orbital angular momentum, and k^2 is the energy in rydbergs of the scattered electron.

The continuum orbital behaves asymptotically:

$$f_{k\ell}(R) \underset{R\to\infty}{\sim} \sin(kR - \frac{\ell\pi}{2} + \eta_{k\ell}) \quad , \tag{17h}$$

where $\eta_{k\ell}$ is the phase shift, which describes the distortion of the wavefunction by the target. We have employed wavefunctions that have the form of Eq. (17h) in all of our deviations of the dipole matrix elements and Gaunt factors. The scattering programs usually produce a solution that behaves asymptotically:

$$f^K_{k\ell}(R) \underset{R\to\infty}{\sim} [\hat{j}_\ell(kR) + \hat{n}_\ell(kR)\, K]k^{-1/2} \quad , \tag{17i}$$

where $\hat{j}_\ell$ ($\hat{n}_\ell$) is the Ricatti-Bessel (Ricatti-Neumann) function of order ℓ and K is the reactance matrix [$= \tan(\eta_\ell)$]. The reactance matrix form can be converted into the behavior of Eq. (17h) by dividing $f^K(R)$ by $[(1+K^2)/k]^{1/2}$.

The interaction potential W is in general nonlocal and energy-dependent and is traditionally divided into two parts:

$$W(R|R') = V_s(R)\,\delta(R-R') + V_e(R|R') \quad . \tag{17j}$$

The first term or static (direct) potential is simply the electrostatic interaction of the target and continuum electron averaged over the ground state of the atom. The second term, or exchange kernel, which is a function of the bound orbitals, arises from the enforcement of the Pauli principle on the total-system wavefunction. For the cases under consideration, the expressions for V_s and V_e are given in Appendix C. Generally, we shall use the SE case as the standard against which we evaluate other models, although we shall augment this formation with model polarization-correlation potentials. Since these potentials mock the virtual transitions to the excited electronic states, they also simulate the distortion of the target by the incident electron.

3. Model Potentials. We shall also consider various approximations of the interaction potential [Eq. (17j)]. In all of these cases, we neglect the exchange kernel and replace V_s by a local, model potential. The following paragraphs present eight models.

(a) Static Interaction.

Point Charge Model

$$V_{PC}(R) = -\frac{Z}{R} \quad , \tag{18}$$

Yukawa or Screened Coulomb Model

$$V_Y(R) = -\frac{Z}{R}\exp(-\lambda R) \quad , \tag{19}$$

Averaged Static Model

$$V_S(\vec{R}) = +\int_0^\infty \rho(\vec{r})|\vec{R}-\vec{r}|^{-1}d\vec{r} - Z_N\, R^{-1} \quad , \tag{20a}$$

where

$$\rho(\vec{r}) = \sum_{i=1}^{n_o} n_i |\varphi_i(\vec{r})|^2 \quad , \tag{20b}$$

φ_i is a bound orbital of the target system, Z_N is the nuclear charge, n_i is the occupation number, and n_o is the number of occupied orbitals. For a closed-shell target or for an atom with a single s-electron outside a closed shell, the static potential given by Eq. (20a) is exact. For other systems, the average implied in Eq. (20a) forms an approximation to the actual direct potential. When the orbitals of the neutral system are used to represent the ion, we term this the frozen-core (FC) approximation.

For an ionic system, we introduce plasma-screening effects into the static potential with the following construction:

Screened Static (SS) Model

$$V_{SS}(R) = \begin{cases} V_S(R) & R \leq R_o \\ -Z_r R^{-1} \exp[-\lambda_D(R - R_o)] & R > R_o \end{cases} \quad , \tag{20c}$$

where λ_D is the inverse of the Debye length (ℓ_D) and Z_r is the residual ionic charge. For example, for Al^+, Z_N in Eq. (20a) will be 13.0 while Z_r will be 1.0. This is a crude model of plasma screening but gives some indications of the trends.

(b) Exchange. We introduce exchange effects through a local, energy-dependent, free-electron gas[21,22] potential:

Free-Electron Gas (FEG) Model

$$V_{FEG}(\vec{R}) = V_S(\vec{R}) + V_{ex}(\vec{R}) \quad , \tag{21a}$$

where V_S is given by Eq. (20a),

$$V_{ex}(\vec{R}) = \pm \frac{2}{\pi} k_F(\vec{R}) \left[\frac{1}{2} + \frac{1-\eta^2}{4\eta} \ln\left(\frac{1+\eta}{1-\eta} \right) \right] \quad , \tag{21b}$$

and the plus (minus) sign at the beginning of the right-hand expression indicates singlet (triplet) scattering. The Fermi momentum has the form

$$k_F(\vec{R}) = [\alpha\pi^2 \rho(\vec{R})]^{1/3} \quad ,$$

where ρ is given by Eq. (20b) and α is 3 (6) depending on whether the target has a closed (open) valence shell. The parameter η is constructed as

$$\eta = (k^2 + I + k_F)^{1/2}/k_F \quad , \tag{21c}$$

where k^2 is the scattering energy of the electron in rydbergs and I is an effective ionization potential of the target. This form is termed the Hara free-electron gas-exchange (HFEGE) potential.[21] Riley and Truhlar suggest a modification in which the ionization potential is set to zero (I = 0). Because of its behavior, this modification is designated the asymptotically adjusted free-electron gas-exchange (AAFEGE) model.

For Eq. (20a) and Eq. (20c) and for Eqs. (21a) - (21c), we have represented the static (S) potentials in terms of the vector variable $\vec{R}$, which has both radial and angular components [$\vec{R} \equiv (R, \theta, \varphi)$]. We derive a radial equation as in Eq. (17g) from the vector Schrödinger equation by (1) invoking a single-center expansion of the continuum wavefunction, the bound wavefunction, and the potential in terms of spherical harmonics $Y_{\ell m}(\hat{R})$; (2) multiplying through by $Y^*_{\ell' m'}(\hat{R})$; and (3) integrating over all angular coordinates [see Eqs. (17d) - (17f)].

(c) **Polarization—Correlation.** The above-mentioned model potentials are approximations to the SE interaction term W. If we wish to go beyond the SE level for elastic scattering, we must include correlation-polarization effects. These effects arise from virtual excitations of the target atom and result in an additional nonlocal, energy-dependent term in Eq. (17f).

We employ two models for the polarization-correlation interaction. The first is simply the asymptotic form truncated at some small radial value within the charge cloud of the target in order to satisfy the proper behavior at the origin:

Cut-off Polarization Potential (SEP1a) Model

$$V_{P1}(R) = \frac{-\alpha}{2R^4}[1 - \exp[-(R/R_o)^6]] \quad , \tag{22a}$$

where α is the dipole polarizability of the target atom. We adjust the parameter R_o to make the phase shifts agree as closely as possible with those of more elaborate scattering calculations. When the whole cutoff term is raised to the sixth power with the exponential coefficient reduced to linear dependence, we term the model SEP1b.

The second model is based on an FEG treatment much the same as the exchange term:

FEG Polarization Potential (SEP2) Model

$$V_{P2}(R) = \begin{cases} V_{corr}(R) & r < R_o \\ V_{P1}(R) & r \geq R_o \end{cases} \quad , \tag{22b}$$

where V_{corr} is the FEG coorelation potential[27,28] and V_{P1} is given by Eq. (22a). The matching point R_o is selected so that the two forms merge smoothly. This polarization potential, unlike SEP1, has no adjustable parameters.

We have tested our construction of this potential by comparing our results for the rare-gas systems with those of O'Connell and Lane.[27] Since we employ the FEG correlation potential of Perdew and Zunger (see Padial and Norcross[28]), we find slight differences with the above authors, who employed a more attractive form of V_{corr}. For example, we determine matching radii of 1.773, 2.047, and 2.9177 a_o for helium, neon, and argon, respectively, while O'Connell and Lane give radii of 1.67, 1.95, and 2.87 for these elements. We have used the following polarizabilities for this calculation: 1.38 (helium), 2.66 (neon), and 11.00 a_o^3 (argon). These slight differences in the V_{corr} and R_o parameters do not greatly affect the scattering results and lead to s- and p-wave phase shifts that are in excellent agreement.

(d) Other Forms. The models described above are completely self-contained and are treated with computer programs GAUNTBA and GNTLABA. Several other programs, which model the macroscopic properties of a medium, use other schemes for determining the absorption coefficients and Gaunt factors.

MOOP Model

MOOP, which is a locally written program to determine opacities, employs a scaled point-charge form for the Gaunt factor as given by Green[5]

$$\bar{g} = \frac{\sqrt{\pi}}{2I_{1/2}(\alpha)}[S + g_{FD}(\gamma^2, u, \alpha - 2\gamma^2\lambda_D)] \quad , \tag{23}$$

where

$$S = \left(1 - \frac{2\gamma^2}{u}\lambda_D{}^2\right)\left(\frac{g_o}{1 - e^{-u}}\right)\log\left\{\frac{(1 + e^{\alpha})(1 + e^{\alpha - u - 2\gamma^2\lambda_D})}{(1 + e^{\alpha - u})(1 + e^{\alpha - 2\gamma^2\lambda_D})}\right\} \quad ,$$

g_{FD} is the Gaunt factor for a point charge Ze averaged over a Fermi-Dirac distribution, λ_D is the inverse Debye length, $\gamma^2 = Z^2/kT$, $u = h\nu/kT$, α is the degeneracy parameter, and g_o is the asymptotic value of the point-charge Gaunt factor (E = 0). The Gaunt factor for a point-charge is given by Karzas and Latter,[4] and the values of g_{FP} and $2I_{1/2}^{(\alpha)}/\sqrt{\pi}$ ($= g_{FD}/\bar{g}$) can be obtained from tables by Green.[5]

XSNQ Model

The XSNQ package,[18] a nonlocal-thermodynamic-equilibrium emission and absorption coefficient subroutine, also employs a scaled point-charge form for the Gaunt factor. The scaling is in terms of an effective charge Z^{*o}, which is given by Eq. (3.2) of Ref. 18. For a neutral system, Z^{*o} is zero, clearly leading to an incorrect representation of the Gaunt factor.

4. Method of Solution. We employ two methods to determine the solution of Eq. (17g): (1) the iterative integral equations (IIE) method[23] and (2) the linear algebraic (LA) method.[20,24] Both methods provide highly accurate solutions of the Schrödinger equation and give Gaunt factors within a few percent of each other. In the remainder of this section, we present a brief description of each procedure.

(a) Iterative Integral Equations Method. For the IIE exposition, we rewrite Eq. (17g) as

$$\hat{L}f(R) = X(R|f) \quad . \tag{24a}$$

where

$$\hat{L} = L - V_s(R) \quad , \text{and} \tag{24b}$$

$$X(R|f) \equiv \int V_e(R|R')\, f(R')\, dR' \quad . \tag{24c}$$

To start the iterative process, we solve the homogeneous equation

$$\hat{L}f^0(R) = 0$$

and term this solution the zeroth iterate. We now substitute f^0 into Eq. (24c) and determine $X(R|f^0)$. Since both the exchange kernel and the wavefunction are known, the expression for X behaves like a local potential. We then use this "potential" to construct the next iterate:

$$\hat{L}f^1(R) = X(R|f^0) \quad . \tag{25b}$$

We continue this scheme by the prescription

$$\hat{L}f^n(R) = X(R|f^{n-1}) \tag{25c}$$

until the phase shifts from successive iterations agree to within a specified tolerance.

The actual form of the scattering equation at each iteration involves only a local potential. This can be seen more readily by making the identification

$$f^n(R)/f^{n-1}(R) \sim 1 \quad , \tag{26a}$$

which is valid for a converged function, and by substituting it into Eq. (25c) to obtain

$$[L + V_{n-1}(R)]\, f^n(R) = 0, \tag{26b}$$

where

$$V_{n-1}(R) \equiv \frac{X(R|f^{n-1})}{f^{n-1}(R)} - V_s(R) \quad .$$

We solve Eq. (26b) by an integral equations (IE) algorithm. We first convert the differential form to an integral equation by employing the free-particle Green's function $G_\ell(R|R')$ such that

$$f_{k\ell}(R) = k^{-1/2}\, \hat{j}_\ell(kR) + \int_0^\infty G_\ell(R|R')\, V_{r\,-1}(R') f_{k\ell}(R') dR' \quad , \tag{27a}$$

where

$$LG_\ell(R|R') = \delta(R - R') \quad , \text{and} \tag{27b}$$

$$L\hat{j}_\ell(kR) = 0 \quad . \tag{27c}$$

The Green's function in this case has a very simple form:

$$G_\ell(R|R') = -\begin{cases} G^1(R)\,G^2(R') & R < R' \\ G^1(R')G^2(R) & R \geq R' \end{cases} \quad , \tag{28}$$

where G_1 is $k^{-1/2}\hat{j}_\ell$ (kR) and G_2 is $k^{-1/2}\hat{\eta}_\ell$ (kR). Substituting Eq. (28) into Eq. (27a) and making several rearrangements of the resulting expression,[23] we can write the solution as

$$f_{k\ell}(R) \equiv G^1(R)I^2(R) - G^2(R)I^1(R) \quad , \tag{29a}$$

where

$$I^m(R) \equiv \delta_{m2} + \int_0^R G^m(R')\, V_{n-1}(R')\, f_{k\ell}(R')dR' \quad . \tag{29a}$$

To effect a propagator solution to Eq. (29a), we introduce a discrete quadrature representation for the functions and integrals and obtain

$$f_{k\ell}(i) = G^1(i)I^2(i-1) - G^2(i)I^1(i-1) \quad , \tag{30a}$$

where

$$I^m(i) \equiv I^m(i-1) + G^m(i)\, V_{n-1}(i) f_{k\ell}(i)\omega_i \quad , \text{and} \tag{30b}$$

ω_i is a quadrature weight. Since the function at step i depends only on the integrals one step back and on known functions at i, the procedure can be employed to propagate the solution outward from the origin [f(0) = 0]. We use a trapezoidal quadrature for this propagation and obtain the K-matrix from the simple relationship

$$K = -I^1(\infty)/I^2(\infty) \quad . \tag{31}$$

(b) Linear Algebraic Method. The LA approach[20,24] does not rely on an iterative prescription and treats the nonlocal term directly. We return to an IE formulation of Eq. (17g) in terms of the free-particle Green's function [Eqs. (27a)–(27c) and Eq. (28)] and write the solution as

$$f_{k\ell}(R) = G^1(R) + \int_0^\infty G(R|R') \int_0^\infty W(R'|R'')\, f_{k\ell}(R'')dR''\, dR' \quad . \tag{32}$$

We now introduce a discrete quadrature for the integrals and functions, and we obtain an equation of the form

$$f_{k\ell}(i) = G^1(i) + \sum_{m=1}^{N} G(i|m)\omega_m \sum_{j=1}^{N} W(m|j)\, f_{k\ell}(j)\omega_j \quad , \tag{33a}$$

where, as before, ω_m and ω_j are weighting functions. We now rearrange Eq. (33a):

$$\sum_j M_{ij}\, f(j) = G^1(i) \quad , \tag{33b}$$

where

$$M_{ij} \equiv \delta_{ij} - \sum_m G(i|m)\, W(m|j)\omega_j\, \omega_m) \quad . \tag{33c}$$

Since all the functions in Eq. (33c) are independent of the solution f, we can evaluate M_{ij} directly. Equation (33b) is in the form of an LA system and can be solved by straightforward matrix methods. This matrix is of order n_p, the number of points in the quadrature mesh. We typically employ a Gauss-Legendre quadrature scheme.

C. Dipole Matrix Elements

Once the continuum functions have been calculated from a prescription in Section II.B, we can evaluate the dipole matrix elements d_{if} in either the length or the acceleration form. For a local, energy-independent potential, both forms should give the same result. This fact provides a convenient check on the numerical prescriptions. For the SE case in which a nonlocal term appears in the potential V, the formulation of the acceleration case is ambiguous, and calculations are usually performed using the length expression. Since the acceleration form involves the derivative of a local potential, which is fairly short-ranged in all of our applications, we employ a straightforward numerical integration of the moment expression.

On the other hand, the dipole-length form accentuates the long-range form of the wavefunctions. In addition, the integration of a pair of oscillating functions with a growing radial term is notoriously unstable. One commonly used procedure is to evaluate the integral as a limit:[10]

$$\lim_{\alpha \to 0} \int_0^\infty e^{-\alpha R} f_1(R)\, R\, f_2(R) dR \quad . \tag{34}$$

This formulation, although cumbersome, is quite stable. Other procedures based on asymptotic expansions have also been employed (see Refs. 29,30).

We take a slightly different approach, based on the matricant method of Knirk,[29] and divide the evaluation of the dipole-length integral into two regions:

$$d = d^{I} + d^{II} \quad , \tag{35a}$$

where

$$d^{I} \equiv \int_0^a f_1(R)\, R\, f_2(R) dR \quad , \tag{35b}$$

and

$$d^{II} \equiv \int_a^\infty f_1(R)\, R\, f_2(R) dR \quad . \tag{35c}$$

The division radius, a, is typically the approximate size of the atomic system. The first term d^{I} is evaluated by a straightforward numerical integration scheme. In the second term d^{II}, we assume that the division radius is sufficiently large that f_1 and f_2 have reached their proper asymptotic forms as given by Eq. (17h). We have thus reduced the evaluation of d^{II} to the integration over known analytical forms, the Ricatti-Bessel and Ricatti-Neamann functions. In Appendix D, we outline the procedure for calculating d^{II}. Once d_{if} is known, we may then evaluate the Gaunt factor and related absorption coefficients.

III. RESULTS AND DISCUSSION

A. Tests of the Programs

We have written two programs, GAUNTBA and GNTLABA, that calculate the averaged Gaunt factor in the IIE and LA methods, respectively. Both programs employ a Gauss-Laguerre quadrature of n_ϵ points to perform the integral in Eq. (8a). The numerical techniques for solving the scattering equations and for constructing the dipole matrix elements and Gaunt factors are given in the previous section (II). We now test these algorithms by comparing them to other calculations.

1. Hydrogen Atom. As a first test, we treat atomic hydrogen at infrared frequencies and at temperatures of a few thousand kelvins at the SE level. We then compare our findings with other results. In the determination of the dipole matrix elements, we make one simplifying approximation by neglecting terms dependent on overlap integrals of the form $\Delta(\varphi_i f_{k\ell})$. These terms are usually quite small compared with the usual dipole form of Eq. (14a). All calculations are performed in the length form; in addition, five energies are used in the averaging prescription. Other parameters are given in the tables. In Table I, we compare our absorption coefficient, corrected for stimulated emission [Eq. (A.16)], to that of John.[8] The agreement is quite good over the whole range of temperatures and frequencies. These

TABLE 1. Comparison of Absorption Coefficients for H^- at the SE Level[a,b]

Δk^2	θ	$\bar{g}_s$	$\bar{g}_t$	$\bar{g}$	κ	κ_E	κ_J	κ_{BKM}
0.05	0.5	4.828(−2)	2.173(−2)	3.287(−2)	1.952	1.060	1.04	
	1.0	3.180(−2)	1.099(−2)	1.620(−2)	2.720	2.152	2.17	2.08
	2.0	2.090(−2)	4.766(−3)	8.799(−3)	4.179	3.997	4.11	3.54
0.10	0.5	7.115(−2)	3.839(−2)	4.658(−2)	0.346	0.274	0.271	
	1.0	5.501(−2)	1.842(−2)	2.757(−2)	0.579	0.554	0.567	0.545
	2.0	4.239(−2)	9.770(−3)	1.792(−2)	1.064	1.062	1.11	0.977
0.20	0.5	1.222(−1)	6.408(−2)	7.860(−2)	0.073	0.070	0.073	
	1.0	1.087(−1)	3.754(−2)	5.532(−2)	0.145	0.145	0.158	
	2.0	9.217(−2)	2.348(−2)	4.065(−2)	0.302	0.302	0.339	

[a]Nomenclature: Δk^2 is the photon energy in rydbergs;
$\theta = 5040/T$ (kelvins);
$\bar{g}_s$ ($\bar{g}_t$) is the averaged Gaunt factor for singlet (triplet) scattering;
$\bar{g} = (3\bar{g}_t + \bar{g}_s)/4$;
κ is the pressure absorption coefficient;
κ_E is this coefficient corrected for stimulated emission, κ_J from Ref. 8 (κ's in units of 10^{-26} cm^4/dyn) and κ_{BKM} from Ref. 31; and
$Z_c = 1$.
[b]Parameters: Calculations performed in the LA approximation with $n_p = 90$ and a mesh /0.0 - 1.0/1.0 - 3.0/3.0 - 10.0/ with 30 points per region;
$\ell_m = 4$; and
$n_e = 5$.

results also agree with the single-channel ("1S") calculations of Doughty and Frazer.[10] We also compare our calculations with those of Bell et al.,[31] which are probably the most accurate free-free calculations to date. These researchers employ both exchange and correlation-polarization effects in the scattering solutions. However, their results are within 20% of the SE for the range under consideration.

2. **Helium Atom.** To investigate the validity of our approach for more complicated systems, we also make comparisons with other calculations for helium and neon. For helium absorption, we invoke the SE approximation and use the near-Hartree-Fock (near-HF), bound 1s-wavefunction of Clementi.[32] In Table 2, we compare our results with those of John[33] and Bell et al.[30] Both groups of authors employ the elastic e-He phase shifts of LaBahn and Callaway,[34] which include both exchange and polarization effects, but each group uses a different asymptotic approximation to determine the dipole matrix elements.

In addition, we present the R-matrix results of Bell et al.[35] These researchers include multichannel effects and perform the dipole integrals without resort to any approximations. Their results should be considered the best to date. The agreement between the extensive coupled-channel calculations and those at the SE level is excellent, indicating that polarization effects are not very important in this regime.

3. **Neon Atom.** In Table 3, we also compare our results for neon with those of Geltmann[36] and John and Williams.[37] John and Williams employ their asymptotic scheme to evaluate the dipole matrix elements and the elastic e-Ne phase shifts of Thompson.[38] Thompson treats exchange exactly and introduces polarization through a Pople-Schofeld model potential. On the other hand, Geltman[36] calculates the continuum wavefunctions from a Hartree-Fock-Slater potential augmented by a cutoff polarization term but calculates the dipole matrix elements by a direct integration. We report results in both the SE and the SEP2 approximations for the scattering. All of our dipole matrix elements are calculated from a direct integration of the length form (see Appendix D) with no asymptotic approximations. Considering the approximations involved, the agreement is quite reasonable.

4. **Yukawa Potential.** In the above comparisons, we have sought to test the SE procedure since this case will be used as a standard with which to compare the other models. Unfortunately, most of the

TABLE 2. Comparison of Free-Free Absorption Coefficients for He^- at the SE Level[a]

Δk^2	θ	$\bar{g}$	κ	κ_E	κ_J	κ_{BKM}	κ_{BBC}
0.03	0.5	1.090(−2)	2.997	1.124	1.12		1.13
	1.0	3.541(−3)	2.753	1.677	1.60	1.59	1.64
	2.0	1.279(−3)	2.811	2.382	2.19	2.14	2.34
0.05	0.5	1.250(−2)	0.742	0.403	0.407		0.415
	1.0	4.481(−3)	0.753	0.595	0.581	0.559	0.600
	2.0	1.840(−3)	0.874	0.836	0.808	0.770	0.842
0.10	0.5	1.703(−2)	0.126	0.100	0.104		0.110
	1.0	7.276(−3)	0.153	0.146	0.154	0.144	0.165
	2.0	3.585(−3)	0.213	0.212	0.238	0.209	0.242

[a]Nomenclature and parameters same as Table 1 except κ_J from Ref. 33, κ_{BKM} from Ref. 30, and κ_{BBC} from Ref. 35 (all κ's in units of 10^{-26} cm^4/dyn); helium wavefunction of Clementi (Ref. 32).

TABLE 3. Comparison of Free-Free Absorption Coefficients for Ne^- at the SE and SEP2 Levels[a]

Δk^2	θ	$\bar{g}$(SEP2)	κ(SE)	κ(SEP2)	κ_E(SEP2)	κ_G	κ_{JW}
0.10	1.008	1.426(−3)	0.645	0.303	0.290	0.452	0.31
0.10	0.504	4.096(−3)	0.538	0.308	0.244	0.362	0.26
0.20	1.008	2.908(−3)	0.132	0.077	0.077	0.114	0.061
0.05	0.504	2.938(−3)	—	1.765	0.964	1.47	1.20

[a]Nomenclature and parameters same as Table 2 except κ(SE) and κ(SEP2) are the uncorrected absorption coefficients in the SE and SEP2 approximations;
all κ's are in units of 10^{-27} cm^4/dyn;
$R_0 = 2.047$;
κ_{JW} refers to Ref. 37 and κ_G refers to Ref. 36;
near-HF neon wavefunction of Clementi (Ref. 32).

earlier calculations were performed at low temperatures and frequencies. To test the higher energy regimes, we compare our calculations of the averaged Gaunt factor for a Yukawa potential [Eq. (19)] with those of Green.[16] These results are presented in Table 4 for a variety of temperatures and photon energies. The agreement is excellent over all regimes, usually better than a few percent. The only case that violates this observation is for $kT = \Delta k^2 = 0.03$ Ry and $\lambda = 0.25$. The two results differ by $\sim$ 10%. However, this energy regime supports a shape resonance in the electron scattering. In the range of such a resonance, the continuum wavefunction can be quite sensitive to the choice of scattering parameters. We have repeated the calculation for a tighter mesh extending to $50a_0$ and have observed a change in $\bar{g}$ of less than 1%.

5. Resonances. Resonances can have a profound effect on the absorption coefficient over a restricted energy range. For electron scattering from an atom or molecule, two basic types of resonances are important: (1) the Feshbach resonance and (2) the shape resonance. The Feshbach resonance is associated with a doubly excited state of the compound system of electron and atom. These resonances are generally very narrow and are therefore usually not important for a neutral system. Of course, the exception arises when absorption in a distinct spectral line, which lies within the resonance width, becomes important. On the other hand, ionic systems support rydberg series of such compound

TABLE 4. Comparison of Averaged Free-Free Gaunt Factors $\bar{g}$ for a Yukawa Potential V_Y.[a,b]

$kT = \Delta k^2$	λ			
	0.10	0.25	0.50	1.00
0.03	0.3806	0.1292	0.0126	0.0226
	0.3845	0.1161	0.0125	0.0224
0.10	0.7452	0.4077	0.1003	0.0926
	0.7437	0.3971	0.0994	0.0910
1.00	1.191	1.024	0.7407	0.5188
	1.215	1.042	0.7226	0.5230
3.00	1.200	1.155	1.006	0.7508
	1.242	1.170	0.9915	0.7685

[a]Nomenclature: upper entry is from present calculation;
lower entry is from Ref. 16;
kT and Δk^2 are in rydbergs;
λ is defined by Eq. (19);
$Z = 1.0$;
$Z_c = 1.0$.

[b]Parameters: LA solution, $n_p = 150$, mesh /0.0 -1.0/1.0 - 3.0/3.0 - 10./10. - 30./ with 30 points in each region except the last, which has 60;
$n_e = 6$;
$\ell_m = 6$.
For $\Delta k^2 = kT$ and $\lambda \leq 0.25$, we have extended the mesh to 50 a_o.

resonance states. While the contribution within a given line remains small, the accumulated effect may be quite pronounced, as has been demonstrated for impact excitation of ions by electrons.[25] To date, this effect has not been studied for free-free processes. We should also note that, owing to the nature of Feshbach resonances, they will only arise within a multistate or close-coupling representation of the scattering equations and thus cannot be extracted from an SE calculation.

Shape resonances, on the other hand, are produced by simple barrier trapping and can exist for any form of local, model potential. The scattering wavefunction and Gaunt factor are very sensitive to the potential parameters in the region of a resonance. The net effect is usually to enhance the Gaunt factor. In Fig. 1, we present calculations of the Gaunt factor $g(E_i,\omega)$ as a function of the incident electron energy E_i for a photon energy of 0.30 Ry and for a Yukawa potential with two choices of λ. A similar case has been treated by Green.[16] The solid curve represents a potential with $\lambda = 0.25$ and clearly supports a pronounced shape resonance at about 0.09 Ry. If we increase the Yukawa potential by about a factor of 2 ($\lambda = 0.50$), we note that the shape resonance disappears (dashed curve). We see the importance of such structures because the Gaunt factor is *enhanced by almost an order of magnitude* in the range of the resonance. However, a note of caution is due: such resonance structures in model potentials may not exist for more sophisticated treatments of the atomic-scattering process. Thus, if we plan to accurately model the free-free absorption from a particular atomic system, we must make sure that our models reproduce the correct scattering profile and do not introduce spurious shape resonances, which could drastically alter the Gaunt factor over a particular energy range. One additional point is worth noting: averaging over a Boltzmann distribution will usually smooth out the resonance structure to some degree.

B. Comparison of Models

In this section, we compare the various models discussed in Section II.B for several atomic species.

1. Rare Gases. In Table 5, we present the averaged free-free Gaunt factor for helium as a function of the photon energy Δk^2(Ry) and the electron temperature k_BT(Ry) for the following models: SE,

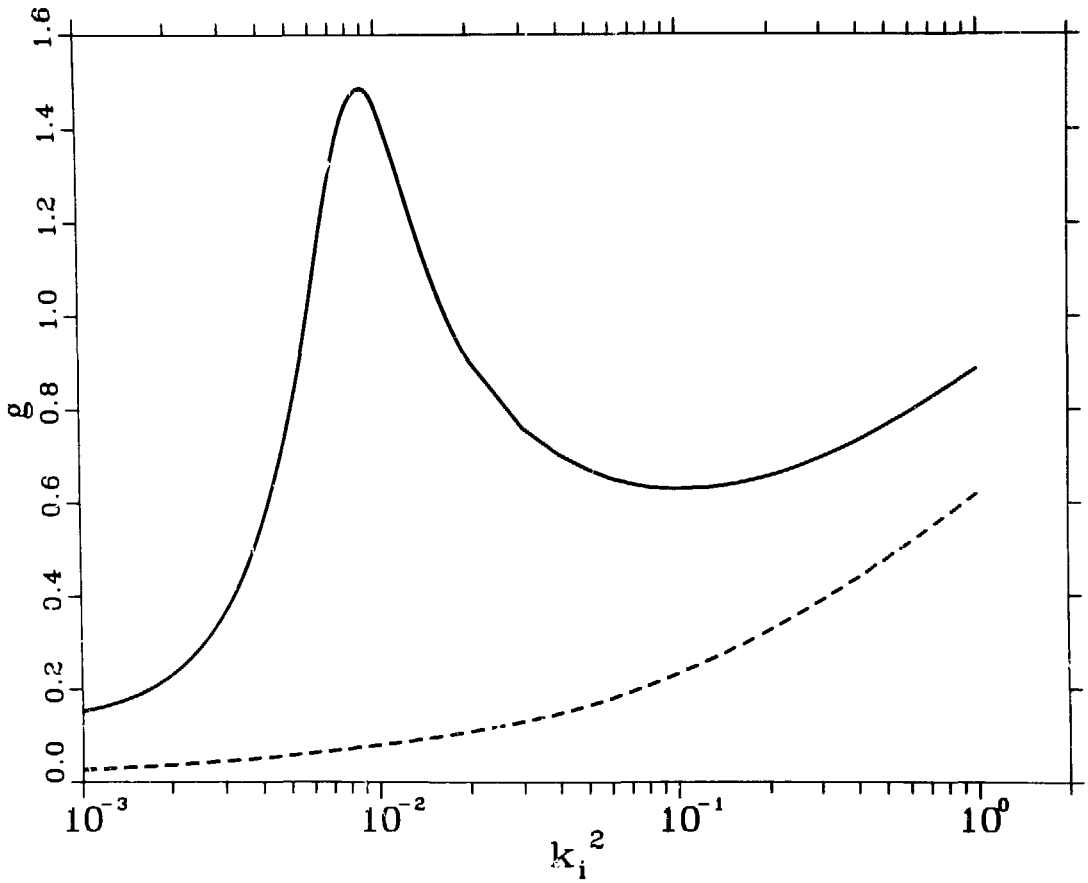

Fig. 1. Gaunt factor $g(k_i^2,\omega)$ as a function of incident electron energy k_i^2(Ry) for a photon energy of 0.3 Ry and a Yukawa potential. Solid line (——), $\lambda = 0.25$; dashed line (— —), $\lambda = 0.50$.

TABLE 5. Comparison of Various Models for the Averaged Free-Free Gaunt Factor $\bar{g}$ for He^{+}[a,b]

	$\Delta k^2 = k_B T$			
model	**0.03**	**0.10**	**0.30**	**1.00**
SE	3.215(−3)	3.133(−2)	1.957(−1)	8.561(−1)
AAFEGE	2.939(−3)	3.187(−2)	1.980(−1)	8.697(−1)
HFEGE	4.572(−3)	3.879(−2)	2.107(−1)	8.710(−1)
S	1.618(−2)	8.123(−2)	2.898(−1)	9.049(−1)
SEP2	2.796(−3)	3.183(−2)	2.132(−1)	9.136(−1)

[a] Nomenclature: near-HF helium wavefunctions of Clementi (Ref. 32).

[b] Parameters: LA solution, $n_p = 90$, mesh /0.0 - 1.0/1.0 - 3.0/3.0 - 10./ with 30 points per region;
$\ell_m = 4$;
$n_o = 5$;
Δk^2 ($k_B T$) in rydbergs;
$\lambda = 0.918$ hartrees;
$\alpha_o = 1.38\ a_o^3$ and $R_o = 1.773\ a_o$;
$\Delta E = 19.82$ eV, first excitation threshold.

AAFEGE, HFEGE, S, and SEP2. The calculations were performed with the LA technique and basic parameters are described in the table. We note that both FEG models give very good agreement with the SE over the entire energy regime from 0.03 to 1.00 Ry. On the other hand, the S model overestimates the Gaunt factor by almost a factor of 5 at the lowest energy but agrees to within 10% at the highest energy. The nonadjustable SEP2 model is slightly lower than the SE case at the low energies and slightly higher in the upper energy range. As indicated before, the correlation-polarization effects are not very pronounced for helium below the first excitation threshold of 19.82 eV.

These trends do not hold for neon, as can be seen in Table 6. The HFEGE still gives good agreement with the SE, as does the AAFEGE at the higher energies. However, at the lower energies, the AAFEGE underestimates the $\bar{g}$ by almost a factor of 3. As with helium, the S overestimates the Gaunt factor in the lower range and comes into better agreement at the higher range.

We have also performed calculations with the two model polarization potentials. The cutoff parameter in the SEP1a case was selected to give phase shifts in agreement with those of Thompson,[38] while the SEP2 construction contains no adjustable parameters. The results of both models are considerably smaller than the SE at the lowest energy, indicating the great sensitivity of the Gaunt factor to the scattering formulation employed in this regime. As the energy increases, the SEP1a and SEP2 models come into better agreement between themselves and with the SE results.

In Table 7, we present a similar study for atomic argon Ar^-. In this case, the FEG models bracket the SE result: the AAFEGE is better at low energies and the HFEGE is better at higher energies. The S overestimates for the whole range, whereas the SEP1a model gives the smallest values of $\bar{g}$ for low values of Δk^2 and k_BT. The SEP1a potential was generated to reproduce the low-energy s- and p-wave phase shifts for e-Ar scattering given by Thompson.[38] Except at the very lowest energy, the SE and FEG models appear to give a reasonable representation of the free-free Gaunt factor.

2. Alkali Systems. In Table 8, we compare several of the models presented in Section II.B for the lithium atom (Li). For an alkali, there are two different spin-states, singlet and triplet, that contribute to the final Gaunt factor. In the single-channel approximations for the SE and FEG models, these two spin-states are not coupled, and we may simply add them with an appropriate weight to determine the averaged Gaunt factor. When compared with the SE, the AAFEGE model underestimates the $\bar{g}$ at low energies and overestimates at high energies. The agreement between the SE and FEG approximations is not as good for the alkalis as for the rare gases.

TABLE 6. Comparison of Various Models for the Averaged Free-Free Gaunt Factor $\bar{g}$ for $Ne^{-a,b}$

	$\Delta k^2 = k_BT$			
model	**0.03**	**0.10**	**0.30**	**1.00**
SE	**1.412(−3)**	**1.331(−2)**	**1.230(−1)**	**1.555**
AAFEGE	**4.723(−4)**	**8.826(−3)**	**1.095(−1)**	**1.434**
HFEGE	**1.621(−3)**	**1.535(−2)**	**1.395(−1)**	**1.554**
S	**4.994(−3)**	**5.376(−2)**	**3.495(−1)**	**2.112**
SEP1a	**6.161(−4)**	**8.980(−3)**	**1.167(−1)**	**1.680**
SEP2	**5.856(−4)**	**8.692(−3)**	**1.129(−1)**	**1.662**

[a] Nomenclature same as Table 5 except SEP1a and SEP2; near-HF wavefunction of Clementi (Ref. 32).

[b] Parameters same as Table 5 except $n_p = 120$, mesh /0.0 - 1.0/1.0 - 3.0/3.0 - 20.0/ with 40 points per region; $\alpha_o = 2.66\ a_o^3$, $R_o = 1.75a_o$ for SEP1a, $R_o = 2.047\ a_o$ for SEP2; and I = 0.8505 hartrees; ΔE = 16.62 eV.

TABLE 7. Comparison of Various Models for the Averaged Free-Free Gaunt Factor $\bar{g}$ for Ar^{+a}

	$\Delta k^2 = k_B T$			
model	0.03	0.10	0.30	1.00
SE	2.277(−3)	3.315(−2)	5.250(−1)	4.290
AAFEGE	2.278(−3)	2.718(−2)	5.058(−1)	4.764
HFEGE	2.871(−3)	3.519(−2)	4.593(−1)	4.186
S	1.156(−2)	1.129(−1)	5.600(−1)	3.524
SEP1a	6.519(−4)	3.261(−2)	6.097(−1)	4.373
SEP2	4.150(−4)	3.489(−2)	7.016(−1)	4.540

[a] Nomenclature and parameters same as Table 5 except $\alpha_0 = 11\ a_0^3$, $R_0 = 3.0\ a_0$ for SEP1a, $R_0 = 2.9177\ a_0$ for SEP2;
I = 0.5912 a.u.;
near-HF argon wavefunction of Clementi (Ref. 32);
ΔE = 11.55 eV.

TABLE 8. Comparison of Various Models for the Averaged Free-Free Gaunt Factor $\bar{g}$ for $Li^{+a,b}$

	$\Delta k^2 = k_B T$			
model	0.03	0.10	0.30	1.00
SE				
sing.	2.68(−2)	6.38(−2)	2.08(−1)	1.121(0)
trip.	5.51(−2)	2.85(−1)	8.10(−1)	1.610(0)
ave.	4.80(−2)	2.30(−1)	6.60(−1)	1.488(0)
AAFEGE				
sing.	1.16(−2)	6.59(−2)	2.79(−1)	8.54(−1)
trip.	3.22(−2)	2.42(−1)	1.17(0)	2.56(0)
ave.	2.71(−2)	1.98(−1)	9.44(−1)	2.13(0)
S	2.60(−3)	3.95(−2)	3.12(−1)	1.35(0)

[a] Nomenclature: singlet (sing.), triplet (trip.), spin-averaged (ave.);
near-HF Li wavefunction of Clementi (Ref. 32).
[b] Parameters: LA solution, $n_p = 90$, mesh /0.0 - 1.0/1.0 - 3.0/3.0 - 10.0/ with 30 points per region;
$n_e = 5$;
$\ell_m = 4$;
length form;
ΔE = 1.848 eV.

The low-energy cross sections are profoundly affected by a ^{3}P-shape-resonance, although this is not readily apparent from Table 8. In Fig.2, the ^{3}P-shape-resonance is displayed by its eigenphase sum as a function of incident electron energy. The abrupt rise of the eigenphase sum by nearly a factor of π is a characteristic feature of such a resonance. Although the SE and AAFEGE models have a ^{3}P-shape-resonance, the position and width are not correct when compared with the accurate two-state close-coupling calculation (2CC).[20] Both models place the resonance too high in energy. We have

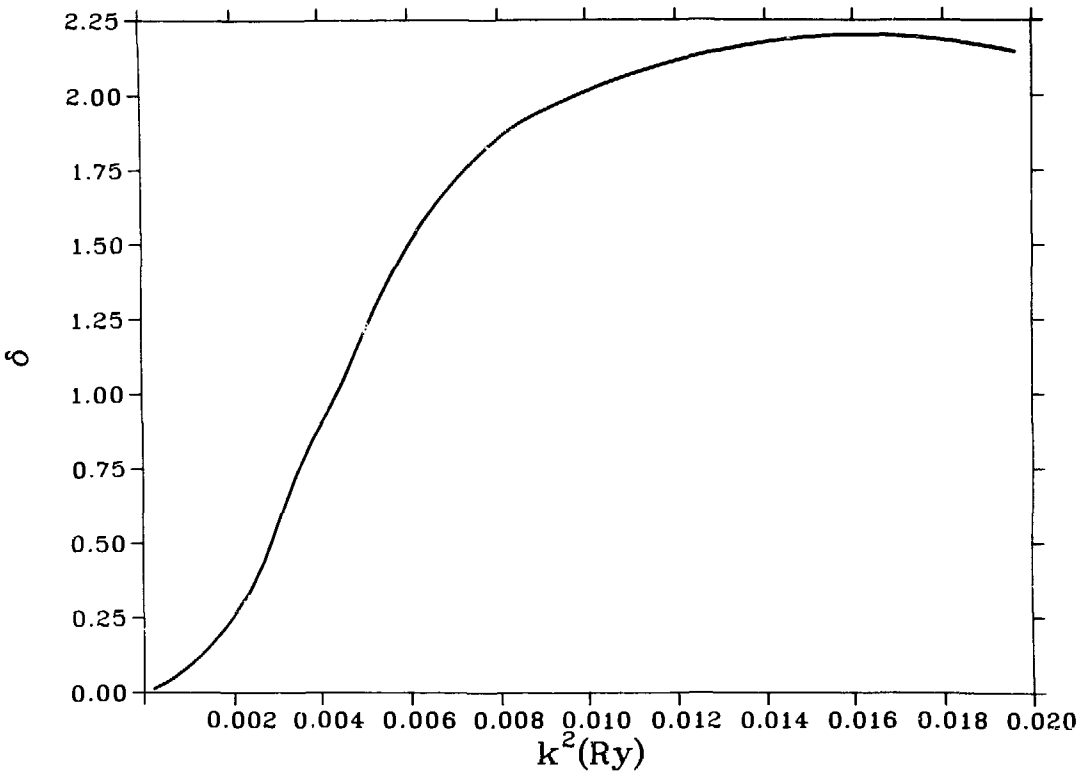

Fig. 2. Eigenphase sum as a function of electron energy for e - Li scattering.

introduced a model cutoff SEPlb potential to lower the position of this feature. We set α_o at $164a_o^3$ and R_o at $4.1a_o$. While this choice does not quite place the ^3P-shape-resonance at the correct energy, the resulting resonance parameters, position and width, are much closer to the 2CC result. In Table 9, we demonstrate the profound effects of this resonance on the Gaunt factor by presenting the results for $\bar{g}$ for the SEP case. By comparing with the SE results of Table 8, we immediately discern the sensitivity of the Gaunt factor to such a resonance.

Finally, in Table 10, we present a similar demonstration for Na^-. The trends are similar to those found for lithium with the AAFEGE slightly underestimating the $\bar{g}$ at both low and high energies. The sodium system also supports a ^3P-shape-resonance in electron scattering at low energies. As in the lithium case, this feature causes the Gaunt factor to be quite sensitive to the model potentials in the energy regime spanned by this resonance.

In the two preceding subsections, we have compared various models of the interaction potential for both rare-gas and alkali systems. We have seen that the averaged Gaunt factor for low photon and electron energies is particularly sensitive to the approximation invoked. This sensitivity is further enhanced by the appearance of a shape resonance in the ^3P channel for both lithium and sodium. These low-energy regimes require very accurate scattering calculations from sophisticated multichannel methods.[19,20] On the other hand, as the electron and photon energies rise, the SE model, the FEG model, and even the S model become appropriate. We should caution, however, that even in these regimes, multichannel, correlation, and resonant effects can be important.

3. Aluminum and Its Ions. We have employed a spherically averaged static potential and an FEG potential to represent the elastic scattering of an electron from neutral aluminum. Since All consists of a single p-electron outside a closed-shell, more than one orbital angular momentum of the continuum electron (ℓ) contributes to a total-system state of LS [$\underset{\sim}{L} = \ell + \underset{\sim}{l}$, S = 0, 1] symmetry. Thus, even in the elastic case, we must solve a set of coupled, radial differential equations. These equations will be nonlocal if exchange and correlation effects are included. In fact, a detailed examination of this system would require the inclusion of excited target states in the solution of the scattering equations. The errors

TABLE 9. Averaged Free-Free Gaunt Factor for Li^- in the SEP1b Approximation[a]

	$\Delta k^2 = k_B T$			
	0.03	0.10	0.30	1.00
sing.	2.002(−2)	3.650(−2)	2.378(−1)	1.236
trip.	1.471(−2)	3.677(−1)	6.980(−1)	1.750
ave.	1.153(−1)	2.849(−1)	5.830(−1)	1.622

[a]Nomenclature and parameters same as Table 8 except the SEP1b model with $\alpha_c = 164\ a_0^3$ and $R_c = 4.1\ a_0$.

TABLE 10. Comparison of Models of the Averaged Free-Free Gaunt Factor $\bar{g}$ for Na^{+8}

	$\Delta k^2 = k_B T$			
model	0.03	0.10	0.30	1.00
SE				
sing.	2.756(−2)	6.601(−2)	1.155(−1)	1.487(0)
trip.	4.903(−2)	1.982(−1)	4.099(−1)	1.685(0)
ave.	4.366(−2)	1.652(−1)	3.363(−1)	1.636(0)
AAFEGE				
sing.	1.422(−2)	7.592(−2)	2.887(−1)	9.744(−1)
trip.	4.799(−2)	2.696(−1)	8.354(−1)	1.788(0)
ave.	3.955(−2)	2.212(−1)	6.987(−1)	1.585(0)
S	3.500(−3)	2.155(−2)	2.414(−1)	2.529(0)

[a]Nomenclature and parameters same as Table 8; near-HF Na wavefunction of Clementi (Ref. 32); $\Delta E = 2.10$ eV.

introduced by considering the simple spherically averaged potential are difficult to gauge. However, John and coworkers[9] have found that the inclusion of excited states generated changes in the free-free absorption coefficient of about 30% for infrared frequencies and for temperatures of 500 to 1000 K (0.05 to 1eV). Such a detailed calculation will have to be consigned to a full-scale research project and would have to be addressed with the atomic R-matrix[19] or linear algebraic programs.[20]

In Tables 11-13, we report Maxwell-Boltzmann-averaged free-free Gaunt factors $\bar{g}_{ff}$ at several electron temperatures and photon frequencies for the various models discussed in Section II. We use $\bar{g}_{ff}$ as a comparative and set Z_c equal to one since all other quantities, such as $\bar{a}$ and $\bar{\sigma}_{eff}$, are directly related to Z_c. These results are valid for a frequency ω above the plasma cut-off ω_p. For aluminum at densities of 10^{-3} to 10^{-4} g/cm^3, ω_p is a few an tenths of an electron volt.

In Table 11, we consider neutral aluminum (Al). The upper part of the table presents a comparison among the Yukawa ($Z = 1$), point charge, S-FC, and AAFEGE models. We feel that the S-FC and AAFEGE results are the most realistic since they employ a more reasonable representation of the target system. The Yukawa results for $Z = 1$ show a marked increase as the scaling parameter λ is decreased. This behavior arises from the introduction of a d-wave ($\ell = 2$) shape resonance in the electron scattering. From comparison with the S-FC and AAFEGE results, we are safe in concluding that such resonance enhancement does not exist for neutral aluminum. However, such resonances can arise for other systems and charge states and can produce rather dramatic changes over a restricted energy region (see Section III.B.2).

TABLE 11. Boltzmann-Averaged Gaunt Factor $\bar{g}_{ff}$ for Al[a,b]

kT(eV)	1.00	1.00	5.00	5.00	10.00	10.00
$\hbar\omega$(eV)	1.17	5.00	1.17	5.00	1.17	5.00
model						
Yukawa (Z = 1)						
λ = 0.25	0.4108	0.9441	0.4968	0.7750	0.6345	0.8385
0.50	0.0691	0.2108	0.2630	0.3966	0.3955	0.5045
1.00	0.0719	0.2498	0.1782	0.2918	0.2583	0.3391
S-FC[c]	0.0618	0.0707	0.1802	0.2276	0.6124	0.7278
AAFEGE[c]	0.0678	0.2064	0.4969	0.7250	1.0742	1.3239
Point Ch.(Z = 1)[d]	1.2503	1.1593	1.3265	1.2930	1.3508	1.3410
MOOP	1.161	1.115	1.20	1.132		
Yukawa (Z = 13)						
λ = 0.25	1.6955	12.151	7.4564	30.4094	15.359	36.946
0.50	0.5170	3.350	2.2278	4.6718	6.2007	12.009
1.00	0.0622	0.1288	0.4111	0.5619	1.5035	1.8873

[a]Since the absorption coefficient is independent of the choice of the charge Z_c in the Kramer's formula (see Sec. I for a discussion), we calculate all models for $Z_c = 1$. The "charge" in the Yukawa model is a scaling parameter, which is selected to represent either the long-range (Z = 1) or short-range (Z = 13) nature of the aluminum potential and is not a measure of the state of ionization of the medium.
[b]Numerial integration (IIE): $n_p = 282$, $r_m = 29.8$, $\ell_m = 10$, $n_e = 10$.
[c]All HF orbitals of Clementi (Ref. 32).
[d]Coulomb-Born: $\ell_m = 10$, $n_{esg} = 10$.

TABLE 12. Boltzmann-Averaged Gaunt Factor $\bar{g}_{ff}$ for Al^{+a}

kT(eV)	1.00	1.00	5.00	5.00	10.00	10.00
$\hbar\omega$(eV)	1.17	5.00	1.17	5.00	1.17	5.00
model						
Point Ch. (Z = 1)[b]	1.2503	1.1593	1.3265	1.2930	1.3508	1.3410
S-FC[c]	1.0024	0.8570	1.4669	1.5060	1.9698	2.1095
SS-FC[c] (R_c=10)						
λ_D=0.10	1.4262	0.8882	1.7719	1.5031	2.2323	2.3226
0.25	1.7683			1.6845		2.4755

[a]Numerical integration (IIE): $n_p = 282$, $r_m = 29.8a_0$, $\ell_m = 10$, $n_e = 10$, $Z_c = 1$.
[b]Coulomb-Born.
[c]All HF orbitals of Clementi.

TABLE 13. Boltzmann-Averaged Gaunt Factor $\bar{g}_B$ for Al^{+3}[a]

kT(eV)	1.00	1.00	5.00	5.00	10.00	10.00
$\hbar\omega$(eV)	1.17	5.00	1.17	5.00	1.17	5.00
model						
Point Ch. (Z = 3)[b]	8.6497	9.4858	8.2718	9.9883	8.783	
S-FC[c]	8.350	8.3074	8.3839	9.8281	8.5021	9.6435
SS-FC[c] (R_o=10)						
λ_D=0.10	10.066	9.7536	10.412	10.753	10.355	11.455
0.25			13.742		8.597	

[a]Numerical integration (IIE): $n_p = 282$, $r_m = 2^{r}$ $?_m = 10$, $n_e = 10$, $Z_c = 1$.
[b]Coulomb-Born.
[c]All HF orbitals of Clementi.

In the latter part of Table 11, we compare these models with the results of MOOP and the results of a Yukawa potential with Z = 13, the nuclear charge of aluminum. We note that MOOP and the point-charge results can be in error by as much as an order of magnitude. The results for the Yukawa potential with Z = 13 are clearly unrealistic because the model leads to an overly strong potential in the intermediate radial range from R ~ $3a_o$ to R ~ $20a_o$. The main point to draw from Table 11 is that for neutral systems the Gaunt factors for low temperatures and photon energies are *very sensitive* to the model employed. If neutral species are present and low-energy regimes are important, then considerably more sophisticated models must be employed to treat these cases.

In Tables 12 and 13, we make similar comparisons for Al^+ and Al^{+3}. For the ion cases, the differences among the various models are less pronounced than for the neutral case. The models differ by approximately a factor of 2, even when plasma-screening effects are invoked. From MOOP we derive a Debye length of approximately $10a_o$ for the temperatures, densities, and radiation fields considered in the tables. Thus, we conclude that if a system has a reasonable population of neutrals, the free-free absorption within a specific line could be in error by a factor of 10 over the standard treatment in current opacity programs. However, for ionic species the absorption is in error by a factor of 2. We emphasize that these differences arise at a particular frequency for a specific line; the *mean* opacities are probably much less in error.

ACKNOWLEDGMENTS

We wish to acknowledge useful conversations with and suggestions from W. Huebner, N. Magee, J. Mann, R. E. H. Clark, N. T. Padial, and N. Delamater.

REFERENCES

1. J. A. Gaunt, "V. Continuous Absorption," *Philos. Trans. R. Soc. London, Ser. A* **229**, 1603 (1930).

2. J. A. Wheeler and R. Wildt, "The Absorption Coefficient of the Free-Free Transitions of the Negative Hydrogen Ion," *Astrophys. J.* **95**, 281 (1942).

3. S. Chandrasekhar and F. H. Breen, "On the Continuous Absorption Coefficient of the Negative Hydrogen Ion III," *Astrophys. J.* **104**, 430 (1946).

4. W. J. Karzas and R. Latter, "Electron Radiative Transitions in a Coulomb Field," *Astrophys. J. Supp.* **6**, 167 (1961).

5. J. Green, "Fermi-Dirac Averages of the Free-Free Hydrogenic Gaunt Factor," Research Memorandum RM-2580-AEC, The Rand Corp. (1960).

6. S. Geltman, "Continuum States of H^- and the Free-Free Absorption Coefficient," *Astrophys. J.* **141**, 376 (1965).

7. T. Ohmura and H. Ohmura, "The Free-Free Transitions of the Negative Hydrogen Ion in the Exchange Approximation," *Astrophys. J.* **131**, 8 (1960).

8 .T. L. John, "The Free-Free Transitions of the Negative Hydrogen Ion in the Exchange Approximation," *Mon. Not. R. Astron. Soc.* **128**, 93 (1964).

9. T. L. John, D. J. Morgan, and A. R. Williams, "The Free-Free Transitions of Li^- by a 'Multichannel Asymptotic Method,' " *J. Phys. B* 7, 1990 (1974).

10. N. A. Doughty and P. A. Fraser, "The Free-Free Absorption Coefficient of the Negative Hydrogen Ion," *Mon. Not. R. Astron. Soc.* **132**, 267 (1966).

11. K. L. Bell, P. G. Burke, and A. E. Kingston, "Free-Free Transitions of an Electron in the Presence of an Atomic System," *J. Phys. B* **10**, 3117 (1977).

12. M. S. Pindzola and H. P. Kelly, "Free-Free Radiative Absorption Coefficient for the Negative Argon Ion," *Phys. Rev. A* **14**, 204 (1976).

13. L. A. Collins and A. L. Merts, "Comparison of Models of the Gaunt Factor for Free-Free Absorption," *J. Quant. Spectrosc. Radiat. Transfer* **26**, 443 (1981).

14. P. I. Richards, "Summary Report on Investigations of Radiative and Chemical Calculations," Technical Operations Research report TO-1362-24 (1966).

15. I. I. Sobelman, *Atomic Spectra and Radiative Transitions* (Springer-Verlag, Berlin, 1977), Chap. 9.

16. J. Green, "Boltzmann Averages of the Free-Free Gaunt Factor in the Screened Coulomb Potential," R and D Associates reports, RDA-TR-4900-007, (1974)

17. H. R. Griem, *Plamsa Spectroscopy* (McGraw-Hill, New York, 1964), p. 488.

18. W. A. Lokke and W. H. Grasbergen, "XSNQ-U-a Non-LTE Emission and Absorption Coefficient Subroutine," Lawrence Livermore Laboratory report UCRL-52276 (1977).

19. K. A. Berrington, P. G. Burke, M. Le Dourneuf, W. D. Robb, K. T. Taylor, and Vo Ky Lan, "A New Version of the General Program to Calculate Atomic Continuum Processes Using the R-matrix Method," *Compu. Phys. Commun.* **14**, 367 (1978).

20. L. A. Collins and B. I. Schneider, "Linear Algebraic Approach to Electronic Excitation of Atoms and Molecules by Electron Impact," *Phys. Rev.* **27**, 101 (1983).

21. M. E. Riley and D. G. Truhlar, "Approximations for the Exchange Potential in Electron Scattering," *J. Chem. Phys.* **63**, 2182 (1975).

22. M. E. Riley and D. G. Truhlar, "Effects of the Pauli Principle on Electron Scattering by Open-Shell Targets," *J. Chem. Phys.* **65**, 792 (1976).

23. .L. A. Collins, W. D. Robb, and M. A. Morrison, "Electron Scattering by Diatomic Molecules: Iterative Static-Exchange Techniques," *Phys. Rev. A* **21**, 488 (1980).

24. L. A. Collins and B. I. Schneider, "Linear-Algebraic Approach to Electron-Molecule Collisions: General Formulation," *Phys. Rev. A* **24**, 2387 (1981).

25. R. E. H. Clark, A. L. Merts, J. B. Mann, and L. A. Collins, "Quantum-Defect and Distorted Wave Theory Applied to the Resonance Contribution of Inelastic Electron Scattering," *Phys. Rev. A* **27**, 1812 (1983) and references therein.

26. I. Percival and M. J. Seaton, "The Partial Wave Theory of Electron-Hydrogen Atom Collisions," *Proc. Cambridge. Philos. Soc.* **53**, 654 (1957).

27. J. R. O'Connell and N. F. Lane, "Nonadjustable Exchange-Correlation Model for Electron Scattering from Closed-Shell Atoms and Molecules," *Phys. Rev. A* **27**, 1893 (1983).

28. N. T. Padial and D. W. Norcross, "Parameter-Free Model of the Correlation-Polarization Potential for Electron-Molecule Collisions," *Phys. Rev. A* **29**, 1742 (1984).

29. D. Knirk, "Method of Treating Long Range Interactions in the Noniterative Integral Equations Formalism," *J. Chem. Phys.* **57**, 4782 (1972).

30. K. L. Bell, A. E. Kingston, and W. A. McIlveen, "The Free-Free Absorption Coefficient of Negative Helium Ion," *J. Phys. B* **9**, 1453 (1975).

31. K. L. Bell, A. E. Kingston, and W. A. McIlveen, "The Total Absorption Coefficient of the Negative Hydrogen Ion," *J. Phys. B* **8**, 358 (1975).

32. E. Clementi, "Tables of Atomic Wavefunctions," *IBM J. Res. Dev.* **9**, 2 (1965).

33. T. L. John, "The Free-Free Transitions of He^-," *Mon. Not. R. Astron. Soc.* **138**, 137 (1968).

34. R. W. LaBahn and J. Callaway, "Elastic Scattering of Low-Energy Electrons from Atomic Helium," *Phys. Rev.* **147**, 28 (1966).

35. K. L. Bell, K. A. Berrington, and J. P. Croskery, "The Free-Free Absorption Coefficient of the Negative Helium Ion," *J. Phys. B* **15**, 977 (1982).

36. S. Geltman, "Free-Free Radiation in Electron-Neutral Atom Collisions," *J. Quant. Spectrosc. Radiat. Transfer* **13**, 601 (1973).

37. T. L. John and A. R. Williams, "The Continuous Absorption Coefficient of Ne^-," *Phys. Lett. A* **43**, 227 (1973).

38. D. G. Thompson, "The Elastic Scattering of Electrons from Nitrogen, Neon, Phosphorous, and Argon Atoms," *J. Phys. B* **4**, 468 (1971).

APPENDIX A
NOTES ON CONVENTIONS

1) Sobelman

Sobelman[15] defines a quantity called an effective cross section $\sigma_{E\omega,E'}$ for free-free absorption:

$$\sigma_{E\omega,E'} = \frac{4\pi^4 e^2 \hbar \omega}{3c\, k^2} \bar{M}_{EE'} \quad [cm^4\, s] \ , \tag{A.1}$$

where

$$\bar{M}_{E,E'} = \sum_{\ell\ell'} \sum_{SL,L'} [(2L+1)(2L'+1)(2S_1+1)^{-1}(2L_1+1)^{-1}(2S+1)] \times \begin{Bmatrix} \ell & L & L_1 \\ L' & \ell' & 1 \end{Bmatrix}^2 \ell_{max}\, \bar{d}_{\ell\ell'}(E|E')^2 \ . \tag{A.2}$$

The target atom is described by an (L_1S_1) state. The total system (atom + e–) is characterized by LS (L'S') for the initial (final) state:

$$\vec{L} = \vec{L}_1 + \vec{\ell}$$

$$\vec{L}' = \vec{L}_1 + \vec{\ell}'$$

where ℓ (ℓ') is the orbital angular momentum of the incoming (outgoing) electron. The 6-j symbol is given by { } above and the dipole matrix element by

$$\bar{d}_{\ell\ell'}(E|E') = \int_0^\infty R_{E\ell}(r)\, r\, R_{E'\ell'}(r) dr \ ,$$

such that

$$R_{E\ell}(r) \underset{r\to\infty}{\simeq} \left(\frac{2m}{\pi k \hbar^2}\right)^{1/2} \sin\left(kr - \frac{\ell\pi}{2} + \eta_{k\ell}\right) \ .$$

Placing this expression in terms of a dipole matrix element for continuum functions that go asymptotically to sin(θ), we have

$$\sigma = \frac{16\pi^2 m^2 e^2 \omega}{3c\hbar^3 k^3 k'} \bar{M}_{kk'} \ . \tag{A.3}$$

Sobelman defines this quantity in terms of the effective semiclassical cross section of Kramer by

$$\sigma = \frac{16\,\pi^3 Z^2 e^6}{3\sqrt{3}\,\omega^3 c \hbar\, m^2 v^2} g_a \ . \tag{A.4}$$

Equating Eqs. (A.3) and (A.4), we can derive an expression for the Gaunt factor as:

$$g_\omega = \frac{\sqrt{3}\,\omega^4 m^2}{Z^2 \pi e^4 k k'} \bar{M}_{kk'} . \tag{A.5}$$

For potential scattering, scattering from a ground-state closed shell, or scattering from a closed shell with one additional s-electron target, we have the relation

$$\bar{M}_{kk'} = 2M ,$$

where M is given by Eqs.(11) and (12). Thus, the two definitions of g are consistent.

Sobelman also defines a continuum absorption coefficient k_ω with units of cm^{-1}:

$$k_\omega = n_e n_i \langle v\, \sigma_{E\omega,E'} \rangle .$$

which is related to the averaged absorption coefficient, $\bar{a}$, by

$$a(T,\omega) = \frac{k_\omega}{n_e n_i} \quad [cm^5] . \tag{A.7}$$

2) Chandrasekhar-Breen and Geltman

In their 1946 paper,[3] Chandrasekhar and Breen define an absorption coefficient $a(k^2; \Delta k^2)$ in units of cm^5 but with most quantities expressed in atomic units. We demonstrate that the absorption coefficient defined in Eqs. (4), (5), and (11) is consistent with that of Chandrasekhar and Breen.

We first address the Gaunt factor in Eq. (11). Using the relationship implied in Eqs. (14a) and (14b), we write the length form of M in terms of the acceleration form as

$$M_L = \omega^{-4} M_A .$$

(Chandrasekhar and Breen use the acceleration form in terms of the potential V in hartrees).

We therefore have the following form for g:

$$g = \frac{2\sqrt{3}}{Z_c^2 \pi k_R k'_R} M_A(V) , \tag{A.8}$$

where we have appended an R to the wavenumber k to indicate rydberg units [if k^2 is in rydbergs then $k_R \equiv (k^2)^{1/2}$]. We now express the Kramer's form σ_K in atomic units by employing the relationships

$$k = mv\,\hbar^{-1}$$

$$k(cm^{-1}) = k_R\, a_o^{-1} , \text{ and} \tag{A.9}$$

$$\hbar\omega\ (\text{ergs}) = (\Delta k^2)\frac{me^4}{2\hbar^2} ,$$

where Δk^2 is the photon energy in rydbergs and a_o is the Bohr radius ($\hbar^2/me^2 = 5.291771 \times 10^{-9}$cm):

$$\sigma_K = \frac{128\,\pi^3\,\alpha\, Z^2 a_o^5}{3\sqrt{3}\,k_R\,(\Delta k^2)^3} , \tag{A.10}$$

where α is the fine structure constant ($e^2/\hbar c$).

The absorption coefficient is then given by

$$a(k_R^2;\Delta k^2) = \frac{256\pi^2\,\alpha\,a_o^5}{3\,k_R^2\,k_R'\,(\Delta k^2)^3}\,M_A(V)\ , \tag{A.11}$$

which agrees with [Eq. (6)] of Chandrasekhar and Breen.

According to Eqs. (6) and (3), we now derive a Maxwell-Boltzmann-averaged absorption coefficient in terms of the effective temperature $\theta = 5040/T$ (kelvins). We first note the following relations:

$$\frac{E}{k_B T} = \frac{k_R^2\,\hbar^2}{2m\,k_B\,a_o^2\,T(^\circ K)} = C_1\theta k_R^2\ ,$$

and

$$f(E)dE = \left(\frac{2}{\pi^{1/2}}\right)\left(\frac{\hbar^3\,a_o^{-3}}{(2mk_B)^{3/2}}\right)\left(\frac{k_R}{T^{3/2}}\right)\exp\left(-E/k_BT\right)d(k_R^2)$$

$$= C_2\,\theta^{3/2}\,k_R\exp\left(-C_1\theta k_R^2\right)d(k_R^2)\ .$$

where $C_1 = 31.32625$, $C_2 = 197.841$, and k_B is the Boltzmann constant. Using these relations together with Eqs. (A.11) and (6), we find

$$\bar{a}_{CB} = \frac{256}{3}\,\pi^2\,\alpha\,a_o^5\,\frac{\theta^{3/2}}{(\Delta k^2)^3}\,\bar{C}_2 I$$

and

$$I \equiv \int_o^\infty \frac{f(k_R^2)M_A}{k_R^2 k_R'}\,d(k_R^2)\ , \tag{A.12}$$

where $f(k_R^2) \equiv 100\,k_R\exp(-C_1\theta k_R^2)$ and $\bar{C}^2 = C_2/100$.

Chandrasekhar and Breen also define an absorption coefficient per unit pressure (P) per atom as

$$\kappa = n_i\,\bar{a}\,P^{-1} \quad [\mathrm{cm}^4/\mathrm{dyn}]\ . \tag{A.13}$$

Using the expression for the pressure of an ideal gas,

$$P = n_i\,k_B T\ , \tag{A.14}$$

and the relation $(k_B T)^{-1} = 1.43704 \times 10^{12}\theta$, we have

$$\kappa = C_3\,\frac{\theta^{5/2}}{(\Delta k^2)^3}\,I\ , \tag{A.15}$$

where $C_3 = 7.251 \times 10^{-29}$. This form also agrees with that of Geltman[6] if we explicitly represent $f(k^2)$, employ the length form $[M_A = (\Delta k^2)^4 M_L/16]$, and note that his asymptotic form is $(1/\pi k)^{1/2} \sin(kr + ...)$. In addition, this expression conforms with that of John.[8] This absorption coefficient can be related to the averaged Gaunt factor $\bar{g}$ [Eq. (7) of John] through the expression

$$\kappa = C_5 Z_c^2 \theta^{3/2} (\Delta k^2)^{-3} \bar{g} \ , \tag{A.16}$$

where $C_5 = 2.099 \times 10^{-28}$. This coefficient is sometimes corrected for stimulated emission by multiplying by a factor $[1 - \exp(-C_1 \theta \Delta k^2)]$.

APPENDIX B
FORMS OF M

We consider the general form of the dipole element given by Sobelman[15] [see Eq. (A.2)]:

$$\bar{M}_{kk'} = \sum_{\ell\ell'} \sum_{S'LL'} (2L + 1)(2L' + 1)(2S + 1)[2L_1 + 1)(2S_1 + 1)]^{-1}$$

$$\times \begin{Bmatrix} \ell & L & L_1 \\ L' & \ell' & 1 \end{Bmatrix}^2 \ell_{max} \, d_{\ell\ell'}(k|k')^2 \ , \tag{B.1}$$

where $d_{\ell\ell'}$ is given by Eqs. (14a) and (14b). We consider several simple cases:

1) Scattering from a ground-state closed-shell atom: $L_1 = 0$, $S_1 = 0$. We have

$$\begin{Bmatrix} \ell L 0 \\ L'\ell' 1 \end{Bmatrix} = \begin{Bmatrix} \ell \ell' 1 \\ L'L 0 \end{Bmatrix} = \frac{[\delta_{\ell L}\delta_{\ell' L'} (-1)^{\ell+\ell'+1}]}{[(2\ell + 1)(2\ell' + 1)]^{1/2}} \ ,$$

and therefore

$$\bar{M}_{kk'} = \sum_{\ell\ell'} \sum_{S} \ell_{max} \, d_{\ell\ell'}(k|k')^2 (2S + 1) \ .$$

However, for $S_1 = 0$, S must be equal to 1/2 and

$$\bar{M}_{kk'} = 2 \sum_{\ell\ell'} \ell_{max} \, d_{\ell\ell'}(k|k')^2 = 2M \ . \tag{B.2}$$

This same expression also arises for scattering from a central potential.

2) Scattering from a ground-state target with a single s-electron outside a closed shell. The target quantum numbers are $L_1 = 0$ and $S_1 = 1/2$, and the values for the total system become

$L = \ell$,
$L' = \ell'$, and
$S = 0$ or 1 .

For this case, we have

$$\bar{M}_{kk'} = \frac{1}{2} \sum_{\ell\ell'} \ell_{max} \, [d^2_{\ell\ell'}(S) + 3 \, d^2_{\ell\ell'}(T)] \ , \tag{B.3}$$

where d(S) [d(T)] is the radial dipole element for singlet [triplet] scattering.

APPENDIX C
SE EQUATIONS

For the case of scattering from a closed-shell target or from a target with a single s-electron outside a closed shell (alkali), the SE-direct and exchange terms have the form

$$V_S^{LS}(R) = \frac{-2Z}{R} + 2 \sum_{i=1}^{n_o} o_i \sum_{\lambda} f_\lambda \, (\ell_i \ell \; \ell_i \ell | L) y_\lambda \, (\varphi_{n\ell_i} \varphi_{n\ell_i} | R) \; , \tag{C.1}$$

and

$$V_e^{LS}(R|R') = 2(-1)^{l-S} \sum_{i=0}^{n_o} \Big\{ (2\varepsilon_i - k^2)\delta_{\ell_i \ell} \; \delta_{n\ell_i} \varphi_{n\ell_i}(R)$$

$$+ \sum_{\lambda} g_\lambda (\ell_i \ell \; \ell_i \ell | L) \; \varphi_{n\ell_i}(R) \frac{r_<^\lambda}{r_>^{\lambda+1}} \; \varphi_{n\ell_i}(R') \Big\} \; , \tag{C.2}$$

where ℓ_i (ℓ) is the orbital angular momentum of the bound (continuum) electron, Z is the nuclear charge, $\varphi_{n\ell_i}$ is the i-th bound orbital with energy ε_i, k^2 is the energy of the continuum electron, $r_>$ ($r_<$) is the maximum (minimum) of (R,R'), and f_λ and g_λ are angular coefficients given by Percival and Seaton.[26] The y_λ term is defined by

$$y_\lambda(AB\,R) = \int_0^\infty A(R') \; B(R') \frac{r_<^\lambda}{r_>^{\lambda+1}} dR' \; . \tag{C.3}$$

We have assumed LS coupling by which the orbital angular momenta and spins of the bound and scattered electrons are coupled according to

$$\vec{L} = \vec{\ell}_i + \vec{\ell} \; , \text{and}$$

$$\vec{S} = \vec{S}_i + \vec{S} \; .$$

The summation over the variable i extends over all occupied orbitals with occupation number o_i.

APPENDIX D
EVALUATION OF d^{II}

We seek a convenient procedure for evaluating d^{II} given by

$$d^{II} = \int_a^\infty f_{k\ell}(R) \; R \; f_{k'\ell'}(R) \, dR \; , \tag{D.1}$$

where $f_{k\ell}$ and $f_{k'\ell'}$ are solutions to the Schrödinger Eq. (17g). Our approach is similar to the matricant technique of Knirk.[29] We assume that the division radius, a, is large enough so that the continuum

functions have achieved their asymptotic form given by Eq. (17i). Substituting this asymptotic expression into Eq. (D.1), we have

$$d^{II} = [M_{21}(\ell k|\ell' k') + K_{\ell'} M_{22}(\ell k|\ell' k') + K_{\ell} M_{23}(\ell k|\ell' k') + K_{\ell} K_{\ell'} M_{24}(\ell k|\ell' k')] , \quad (D.2)$$

where

$$M_{21}(\ell k|\ell' k') = \int_a^\infty \hat{j}_\ell(kR)\, R\, \hat{j}_{\ell'}(k'R) dR ,$$

$$M_{22}(\ell k|\ell' k') = \int_a^\infty \hat{j}_\ell(kR)\, R\, \hat{\eta}_{\ell'}(k'R) dR ,$$

$$M_{23}(\ell k|\ell' k') = \int_a^\infty \hat{\eta}_\ell(kR)\, R\, \hat{j}_{\ell'}(k'R) dR , \text{ and}$$

$$M_{24}(\ell k|\ell' k') = \int_a^\infty \hat{\eta}_\ell(kR)\, R\, \hat{\eta}_{\ell'}(k'R) dR , \quad (D.3)$$

where $\hat{j}$ ($\hat{\eta}$) is the Ricatti-Bessel (Ricatti-Neuman) function.

We evaluate the M elements by expanding the Ricatti functions in terms of sines and cosines and evaluating the resulting multipolar integrals by simple recursion relations. The Ricatti functions can be expanded as

$$\hat{j}_\ell(kR) = \sum_{m=0}^{\ell} [R(\ell m) \sin(kR) + S(\ell m) \cos(kR)] R^{-m} ,$$

and

$$\hat{\eta}_\ell(kR) = \sum_{m=0}^{\ell} [R(\ell m) \cos(kR) - S(\ell m) \sin(kR)] R^{-m} , \quad (D.4)$$

where R(ℓm) and S(ℓm) are known constants. We now substitute Eq. (D.4) into Eq.(D.3) and derive

$$M_{21} = \sum_{m=0}^{\ell} \sum_{m'=0}^{\ell'} [R(\ell m)\ R(\ell' m')\ E_M(kk'|a) + R(\ell m)\, S(\ell' m')\ F_M(kk'|a) + S(\ell m)\, R(\ell' m')\ G_M(kk'|a) + S(\ell m)\ S(\ell' m')\ H_M(kk'|a)]$$

$$M_{22} = \sum_{m=0}^{\ell} \sum_{m'=0}^{\ell'} [R(\ell m)\ R(\ell' m')\ F_M(kk'|a) - R(\ell m)\, S(\ell' m')\ E_M(kk'|a) + S(\ell m)\, R(\ell' m')\ H_M(kk'|a) - S(\ell m)\ S(\ell' m')\ G_M(kk'|a)]$$

$$M_{23} = \sum_{m=0}^{\ell} \sum_{m'=0}^{\ell} [R(\ell m)\ R(\ell' m')\ G_M(kk'|a) + R(\ell m)\, S(\ell' m')\ H_M(kk'|a)$$

$$- S(\ell m)\, R(\ell' m')\ E_M(kk'|a) - S(\ell m)\ S(\ell' m')\ F_M(kk'|a)]$$

$$M_{24} = \sum_{m=0}^{\ell} \sum_{m'=0}^{\ell'} [R(\ell m)\ R(\ell' m')\ H_M(kk'|a) - R(\ell m)\, S(\ell' m')\ G_M(kk'|a)$$

$$- S(\ell m)\, R(\ell' m')\ F_M(kk'|a) + S(\ell m)\ S(\ell' m')\ E_M(kk'|a)] \quad , \qquad \text{(D.5)}$$

where

$$E_M \equiv \int_a^\infty R^{-M+1} \sin(kR) \sin(k'R) dR \ ,$$

$$F_M \equiv \int_a^\infty R^{-M+1} \sin(kR) \cos(k'R) dR \ ,$$

$$G_M \equiv \int_a^\infty R^{-M+1} \cos(kR) \sin(k'R) dR \ ,$$

$$H_M \equiv \int_a^\infty R^{-M+1} \cos(kR) \cos(k'R) dR \ , \quad \text{and}$$

$$M = m + m' \ . \qquad \text{(D.6)}$$

We determine the latter expressions by writing the product trigonometric functions in terms of the summed-angle relationships. Thus, we have

$$E_M = \frac{1}{2} [C_M(k - k'|a) - C_M(k + k'|a)] \ ,$$

$$F_M = \frac{1}{2} [S_M(k - k'|a) + S_M(k + k'|a)] \ ,$$

$$G_M = \frac{1}{2} [- S_M(k - k'|a) + S_M(k + k'|a)] \ , \text{ and}$$

$$H_M = \frac{1}{2} [C_M(k - k'|a) + C_M(k + k'|a)] \quad , \qquad \text{(D.7)}$$

where

$$C_M(K|a) \equiv \int_a^\infty R^{-M+1} \cos(KR) dR \ , \text{ and}$$

$$S_M(K|a) \equiv \int_a^\infty R^{-M+1} \sin(KR)dR \quad . \tag{D.8}$$

By writing out several of these terms explicitly, we can derive a set of recursion relations of the form

$$C_M(K|a) = \frac{-\sin(Ka)}{Ka^{M-1}} + \frac{(M-1)}{K} S_{M+1}(K|a)$$

$$S_M(K|a) = \frac{\cos(Ka)}{Ka^{M-1}} - \frac{(M-1)}{K} C_{M+1}(K|a) \quad . \tag{D.9}$$

We start the sequence at a large value of $M(> \ell + \ell')$, where $C_m \sim S_m \sim 0$, and recur downwards until we have generated all values of M needed in the expansion. To finally place d^{II} in the proper form, we must divide by $[(1 + K_\ell^2)(1 + K_{\ell'}^2)/(kk')]^{1/2}$.

We compare this procedure with the more standard asymptotic limit form. We select a local potential formulation to compare the length and acceleration forms. The asymptotic limit form is given by

$$\hat{d} = \hat{d}_a^{II} + d^I \ , \tag{D.10}$$

where

$$\hat{d}_a^{II} = \lim_{\alpha \to 0} \int_a^\infty e^{-\alpha r} f_{k\ell}(r) r f_{k'\ell'}(r) \, dr \quad . \tag{D.11}$$

For a given choice of α, we directly integrate Eq. (D.11) by standard numerical procedures. We have used the Common Los Alamos Mathematical Software subroutine DQAGIE, which partitions the interval and performs a Gauss-Laguerre integration within each subregion. We take three values of d and fit the integrals $\hat{d}_a^{II}$ to a simple quadratic form $- a_2\alpha^2 + a_1\alpha + a_o$, where a_o gives the zero limit of the partial moment.

In Table D.1, we compare the above two methods for the length form with the acceleration expression for e-Li scattering from the static potential [Eq. (20a)]. The first column lists the values of α while the second column presents the $\hat{d}_a^{II}$ integral for this particular value of α. The third column displays the a_o coefficient ($\hat{d}_o^{II}$) of the quadratic fit to the present moment value and two preceding moment values. We compare this result with the value of the matricant calculation in column four. The inner integration of d^I is given in the fifth column. Finally, we compare the total length expressions ($d^I + d^{II}$) with the acceleration form (multiplied by $2/\Delta k^2$ to give the same units). We note very good agreement among all the methods; the largest difference is 7% between the acceleration and matricant length. We should also note that Eq. (D.11) is very difficult to accurately integrate from the origin (a = o), requiring very small values of α to obtain precise results.

TABLE D-1. Comparison of Various Methods to Determine the Dipole Matrix Elements: e-Li Scattering in the Static Potential

α	$\hat{d}_\alpha^{II}$	$\hat{d}_\alpha^{II}(\infty)$	d^{II}	d^{I}	$\hat{d}$	d	d^{A}
a) $k_1^2 = 0.10$ Ry, $\ell_1 = 1$; $k_2^2 = 0.20$ Ry, $\ell_2 = 0$							
0.0200	145.905						
0.0100	181.959						
0.0050	201.896	223.107					
0.0025	212.325	223.060	233.355	−229.635	−6.575	−6.300	−6.764
b) $k^2 = 0.10$, $\ell_1 = 0$; $k_2^2 = 0.20$, $\ell_2 = 1$							
0.0100	−106.756						
0.0050	−111.001						
0.0025	−112.598	−113.845	−113.756	89.428	−24.813	−24.328	−24.697
c) $k_1^2 = 0.10$, $\ell_1 = 2$; $k_2^2 = 0.20$, $\ell_2 = 1$							
0.0200	94.939						
0.0100	109.326						
0.0050	115.860	121.953					
0.0025	118.869	121.707	121.638	−103.418	18.289	18.220	18.256
d) $k_1^2 = 1.0$, $\ell_1 = 1$; $k_2^2 = 2.0$, $\ell_2 = 0$							
0.2000	14.1750						
0.0100	17.9452						
0.0050	20.1559	22.584					
0.0025	21.3515	22.607	22.748	26.597	−3.9897	−3.8496	−3.9989